

Two-Equation Thermal Model for Heat Transfer Predictions

Pascale Kulisa, Nathalie Marciniak

Laboratoire de Mécanique des Fluides et d'Acoustique-LMFA-UMR5509
Ecole Centrale de Lyon
BP 163
69131 ECULLY Cedex
France

Notations

k	turbulent kinetic energy	U, u	mean and fluctuating velocity
k_θ	temperature variance	uv	Reynolds stress
Prt	turbulent Prandtl number	$v\theta$	normal turbulent heat flux
P	pressure	y^+	dimensionless coordinate
q_i	heat flux	α_t	turbulent thermal diffusivity
R	time scales ratio	ε	dissipation rate of k
R_t	turbulent Reynolds number	ε_θ	dissipation rate of k_θ
T, θ	mean and fluctuating temperature	τ	kinematic time scale
t	time	τ_θ	thermal time scale

Introduction

The very high temperature level reached in actual turbine components requires accurate simulation tools to predict the heat transfers. The turbine flow is very complex. It is dominated by high pressure gradients, three-dimensional viscous effects, and high heat fluxes. Moreover, the turbulence plays a major role in the heat transfer level. Very efficient turbulence models have been developed for the prediction of dynamic flows. Modélisation of thermal field is relatively inferior to the modelling of dynamic field. The current practice is to use assumption of constant turbulent Prandtl number. The objective of this work is to develop and assess thermal flux models for turbine aerothermal field prediction [1].

Physical model

The physical model is based on the three-dimensionnal compressible Favre averaged Navier-Stokes equations. The equations are written in a conservative form for cartesian coordinates.

Continuity equation :

$$\frac{\partial \rho}{\partial t} + \frac{\partial \rho U_i}{\partial x_i} = 0$$

Momentum equations :

$$\frac{\partial \rho U_i}{\partial t} + \frac{\partial \rho U_i U_j}{\partial x_j} = -\frac{\partial P_s}{\partial x_i} + \frac{\partial \sigma_{ij}}{\partial x_j} - \frac{\partial \overline{\rho u_i u_j}}{\partial x_j}$$

Energy equation :

$$\frac{\partial \rho E}{\partial t} + \frac{\partial \rho E U_i}{\partial x_i} = \frac{\partial \tau_{ij} U_j}{\partial x_i} - \frac{\partial q_i}{\partial x_i} - \frac{\partial \overline{\rho u_i e}}{\partial x_i}$$

where U_i , ρ , P and μ are respectively the velocity, the density, the pressure and the viscosity.

Report Documentation Page

Form Approved
OMB No. 0704-0188

Public reporting burden for the collection of information is estimated to average 1 hour per response, including the time for reviewing instructions, searching existing data sources, gathering and maintaining the data needed, and completing and reviewing the collection of information. Send comments regarding this burden estimate or any other aspect of this collection of information, including suggestions for reducing this burden, to Washington Headquarters Services, Directorate for Information Operations and Reports, 1215 Jefferson Davis Highway, Suite 1204, Arlington VA 22202-4302. Respondents should be aware that notwithstanding any other provision of law, no person shall be subject to a penalty for failing to comply with a collection of information if it does not display a currently valid OMB control number.

1. REPORT DATE 00 MAR 2003	2. REPORT TYPE N/A	3. DATES COVERED -			
4. TITLE AND SUBTITLE Two-Equation Thermal Model for Heat Transfer Predictions		5a. CONTRACT NUMBER			
		5b. GRANT NUMBER			
		5c. PROGRAM ELEMENT NUMBER			
6. AUTHOR(S)		5d. PROJECT NUMBER			
		5e. TASK NUMBER			
		5f. WORK UNIT NUMBER			
7. PERFORMING ORGANIZATION NAME(S) AND ADDRESS(ES) NATO Research and Technology Organisation BP 25, 7 Rue Anelle, F-92201 Neuilly-Sue-Seine Cedex, France		8. PERFORMING ORGANIZATION REPORT NUMBER			
9. SPONSORING/MONITORING AGENCY NAME(S) AND ADDRESS(ES)		10. SPONSOR/MONITOR'S ACRONYM(S)			
		11. SPONSOR/MONITOR'S REPORT NUMBER(S)			
12. DISTRIBUTION/AVAILABILITY STATEMENT Approved for public release, distribution unlimited					
13. SUPPLEMENTARY NOTES Also see ADM001490, presented at RTO Applied Vehicle Technology Panel (AVT) Symposium held in Leon, Norway on 7-11 May 2001, The original document contains color images.					
14. ABSTRACT					
15. SUBJECT TERMS					
16. SECURITY CLASSIFICATION OF:			17. LIMITATION OF ABSTRACT UU	18. NUMBER OF PAGES 6	19a. NAME OF RESPONSIBLE PERSON
a. REPORT unclassified	b. ABSTRACT unclassified	c. THIS PAGE unclassified			

These equations are implemented in the Navier-Stokes code CANARI, developed by ONERA [2]. The equations are discretised in space with a central finite volume scheme associated with a four step Runge-Kutta time scheme. Second and fourth order dissipative terms are added to ensure numerical stability. An implicit smoothing residual could be used to accelerate the convergence.

Turbulence modelling

To close the momentum equations, the Reynolds stresses $\overline{u_i u_j}$ have to be determined. The classical Boussinesq hypothesis is postulated which links the unknown Reynolds stresses to the known velocity field with the turbulent eddy viscosity μ_t . Based on a dimensional analysis, the modelisation of μ_t is built with a velocity scale and a time scale. The turbulent kinetic energy k and its dissipation rate ε are used to express these two scales and μ_t . The two transport equations of k and ε are solved. Damping functions of Hattori-Nagano-Tagawa [3] are introduced to solved the equations up to the wall.

Thermal flux models

The turbulent thermal model is based on a two-equation model. Similar to the modelling of the Reynolds stresses, the thermal fluxes are linked to the mean temperature gradient by a scalar : the turbulent diffusivity α_t . A dimensional analysis is carried out to express α_t . This quantity has the same dimension as μ_t . The most representative velocity scale is that of the turbulent phenomenon, so the root of the kinetic energy is chosen. The time scale is expressed as a product of the velocity time scale $\tau = k/\varepsilon$ and the thermal time scale $\tau_\theta = k_\theta/\varepsilon_\theta$. k_θ is the temperature variance and ε_θ its dissipation rate.

$$\alpha_t = C_\lambda f_\lambda \rho k \sqrt{\tau} \sqrt{\tau_\theta}$$

This kind of model signifies that the kinematic and the thermal phenomena are coupled and the k - ε - k_θ - ε_θ equations are solved simultaneously [4], [5], [6]. The k_θ - ε_θ equations are developed for incompressible flows but on the Morkovin hypothesis [7] they could be adapted to compressible flows if the Mach number fluctuations are small compared to the mean Mach number value.

In the k_θ -equation, the only term to be modeled is the turbulent diffusion and a gradient type representation (like for the k -equation) is used. Various models have been proposed for the ε_θ -equation. The model we implement has two production terms and two destruction terms. For the turbulent diffusion term, a gradient approach is adopted.

The low-Reynolds number model of Hattori-Nagano-Tagawa [3] has been chosen because it solves the pseudo-dissipation ε_θ' transport equation, which allows zero-value at the wall. The use of this variable implies the introduction of additional terms : $(\partial\sqrt{k_\theta}/\partial x_i)^2$ and E_θ .

The modelling equation of k_θ is :

$$\underbrace{\frac{\partial \rho k_\theta}{\partial t}}_{convection} + \underbrace{\frac{\partial \rho U_i k_\theta}{\partial x_i}}_{production} = \underbrace{-\rho u_i \theta \frac{\partial T}{\partial x_i}}_{diffusion} + \underbrace{\frac{\partial}{\partial x_i} \left[\left(\alpha + \frac{\alpha_t}{\sigma_\theta} \right) \frac{\partial k_\theta}{\partial x_i} \right]}_{diffusion} - \underbrace{\rho \varepsilon'_\theta - \left[\frac{\partial \sqrt{k_\theta}}{\partial x_i} \right]^2}_{dissipation}$$

The modelling equation of ε_θ' is :

$$\underbrace{\frac{\partial \rho \varepsilon'_\theta}{\partial t}}_{convection} + \underbrace{U_i \frac{\partial \rho \varepsilon'_\theta}{\partial x_i}}_{production} = \underbrace{C_{p1} f_{p1} \frac{\rho \varepsilon'_\theta}{\rho \theta^2} P_\theta + C_{p2} f_{p2} \frac{\varepsilon'_\theta}{k} P + E_\theta}_{production} + \underbrace{\frac{\partial}{\partial x_i} \left[\left(\alpha + \frac{\alpha_t}{\sigma_\theta} \right) \frac{\partial \varepsilon'_\theta}{\partial x_i} \right]}_{diffusion} - \underbrace{C_{d1} f_{d1} \frac{\rho \varepsilon'_\theta}{\rho \theta^2} \rho \varepsilon'_\theta - C_{d2} f_{d2} \frac{\varepsilon'_\theta}{k} \rho \varepsilon'_\theta}_{destruction}$$

where :

$$f_{p1}, f_{p2}, f_{d1}=1, \sigma_\phi, \sigma_\theta=1, P = -\overline{\rho u_i u_j} \frac{\partial U_i}{\partial x_j}, P_\theta = -\overline{\rho u_i \theta} \frac{\partial T_i}{\partial x_i}$$

$$f_\mu = \left[1 - \exp\left(-y^+/30\right)\right]^2 \left[1 + \frac{20}{R_t^{3/4}} \exp\left[-(R_t/120)^2\right]\right]; E_\theta = \frac{\alpha}{\rho} \alpha_t (1 - f_{\varepsilon\theta}) \left[\frac{\partial^2 T}{\partial x_i \partial x_i}\right]^2$$

$$f_\lambda = \left[1 - \exp\left(-\frac{y^+}{30}\right)\right] \left[1 - \exp\left(-\frac{y^+ P_r^{1/3}}{30}\right)\right] \left[1 + \frac{7.9}{R_t^{3/4}} \exp\left(-\left(\frac{R_t}{120}\right)^2\right)\right]$$

$$f_{d2} = (1.9 f_{\varepsilon 2} - 1)/0.9; f_{\varepsilon\theta} = \left(1 - \exp\left(-y^+ P_r^{1/3}/30\right)\right)^2$$

Channel test case

This test case is a wall-bounded shear flow with thermal gradients. The results of the calculation are compared to the Direct Numerical Simulations of Kasagi [8]. A constant wall heat flux is applied, and the Reynolds number based on the friction velocity and the half height of the channel is $Re=150$. The buoyancy effects are neglected. The grid contains 200 points in the axial direction and 60 points in the normal to the wall direction. The first node is located at $y^+=0.05$.

The mean velocity and temperature distributions are presented figures 1 and 2. For these two quantities, the model shows a good behaviour. In particular at the wall, the results are very satisfactory. Figure 3, the calculated Reynolds stress shows very good agreement with the DNS data. The same remark may be made for the turbulent heat flux, figure 4. The ratio of the thermal and dynamic time scales, R , is presented figure 5. Its evolution is qualitatively reproduced by the two-equation model. We can remark that R is not constant as implied by a constant Prt model.

Turbine blade test case

A turbine stator blade is now tested. The experimental facility is a linear transonic cascade investigated at the Von Karman Institute [9], [10]. The Mach number is 0.151 at the inlet and 0.85 at the outlet. The stagnation temperature of the flow equals 416.8K. The wall is heated at $T_w=296.25K$. The turbulence intensity at the inlet is 4%.

A multi-domain H-O-H grid is used. The upstream H grid contains $9 \times 49 \times 2$ points. A O-type grid is defined around the blade to ensure a good description of the wall boundary layers. The nodes distribution is $301 \times 65 \times 2$, and the first point is located at $y^+=1$. The downstream H-type grid contains $189 \times 49 \times 2$ nodes.

The heat transfer coefficient H along the blade is available and compared to the experimental data, figure 6. On the suction side ($s/s_0 > 0$), the heat transfer coefficient is high near the stagnation point. Up to 20% of the curvilinear abscissa, H decreases, due to the effect of the acceleration on the laminar boundary layer. The calculation results are in good agreement with the experimental data. At $s/s_0 \approx 0.25$, a change in the velocity gradient induced the beginning of the laminar-turbulent transition of the calculated flow. The transition produced the strong increase of the heat transfer coefficient. In the experiment, the laminar-turbulent transition appends more downstream and the increase of H is delayed. The $k-\varepsilon$ model is unable to simulate precisely the transition position. When the transition is completed, H decreases slowly up to the trailing edge. Along this region, the heat transfer level is well predicted by the computation.

On the pressure side ($s/s_0 < 0$), the acceleration of the laminar boundary layer induced the decrease of H . At $s/s_0 = -0.1$, a small separation bubble occurs and initiates the laminar-turbulent transition. These two phenomena produce the increase of the heat transfer level. Qualitatively, the calculation predicts evolutions in agreement with the experimental ones. But the transition is induced too late by the simulation. Downstream, the heat transfer coefficient increases up to the trailing edge. This increase is limited by the effect of the acceleration in this region. The computation seems to be unable to account this effect and overestimates the H level.

Concluding remarks

A two-equation model for the turbulent thermal field has been implemented, in addition of a $k-\epsilon$ model for the dynamic field. These four-equation model has been developed in a Navier-Stokes code. This approach is more universal and avoids to introduce the assumption of a constant turbulent Prandtl number which is not valid when strong temperature gradients exist.

The model is validated for a channel flow. The results are very satisfactory. The heat fluxes are well predicted. A turbine cascade flow is simulated. The physical phenomena are reproduced by the model. Although, the position of the laminar-turbulent transition is not correctly predicted by the code and induced some discrepancies in the heat transfer level. However, the capability of solving this sophisticated closure model in a full Navier-Stokes code, for complex turbine flows, is demonstrated.

References

- [1] N. Marciniak, Modélisation aérothermique à bas nombre de Reynolds des écoulements en turbines, Thèse de Doctorat, Ecole Centrale de Lyon, 1997.
- [2] A.M. Vuillot, V. Couaillier, N. Liamis, 3d turbomachinery Euler and Navier-Stokes calculation with multidomain cell-centered approach, AIAA paper 93-2576 (1993).
- [3] H. Hattori, Y. Nagano, M. Tagawa, Analysis of turbulent heat transfer under various thermal conditions with two-equation models, in : Engineering Turbulence Modelling and Experiments 2, Elsevier publishers, 1993, pp. 43-52.
- [4] Y. Nagano, C. Kim, A two-equation model for heat transport in wall turbulent shear flows, Journal of Heat Transfer 110 (1988).
- [5] T.P. Sommer, R.M.C. So, Y.G. Lai, A near-wall two-equation model for turbulent heat fluxes, Int. Journal of Heat and Mass Transfer 35 (1992).
- [6] M.S. Youssef, Y. Nagano, M. Tagawa, A two-equation model for predicting turbulent thermal fields under arbitrary wall thermal conditions, Int. Journal of Heat and Mass Transfer 35 (1992).
- [7] M.W. Morkovin, Effects of compressibility on turbulent flow, The mechanics of turbulence, CNRS, Paris, 1962.
- [8] N. Kasagi, Y. Tomita, A. Kuroda, Direct numerical simulation of passive scalar field in a turbulent channel flow, Journal of Heat Transfer 114 (1992).
- [9] T. Arts, A. Bourguignon, Thermal effects of a coolant film along the suction side of a high pressure nozzle guide vane, AGARD CP 527, Heat transfer and cooling in gas turbine, 1992.
- [10] T. Arts, I. Lapidus, Behaviour of a coolant film with two rows of holes along the pressure side of a high-pressure nozzle guide vane, Journal of Turbomachinery, vol. 112, 512-521, 1990.

Figures

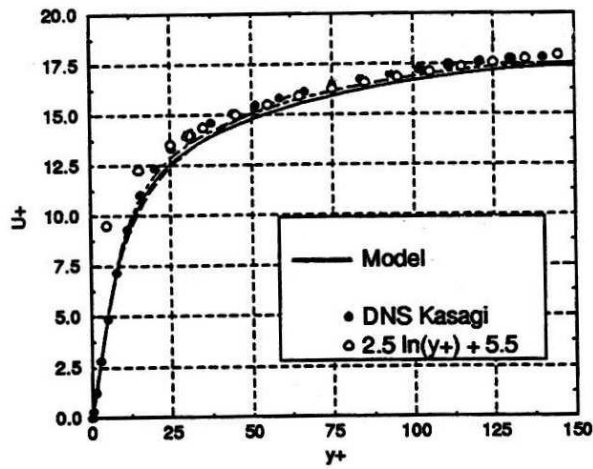


Fig. 1 : Dimensionless velocity profile U^+

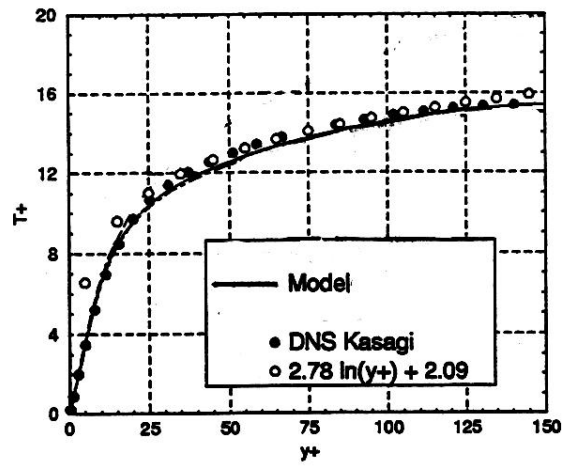


Fig. 2 : Dimensionless temperature profile T^+

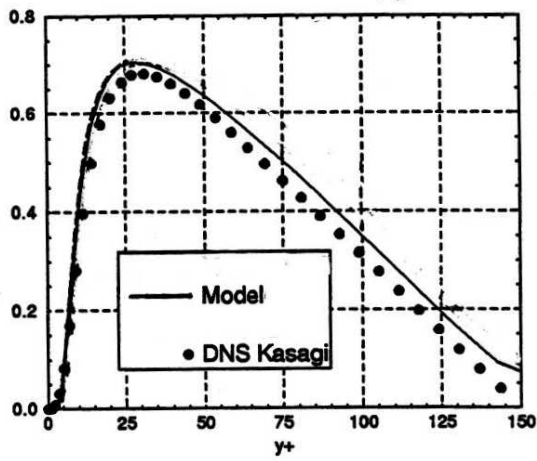


Fig.3 : Dimensionless Reynolds stress $-uv^+$

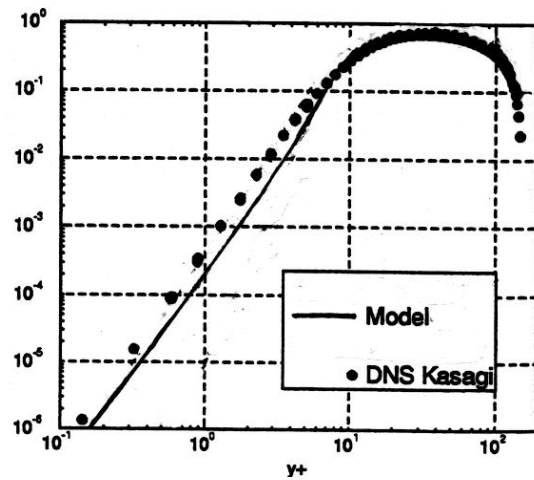


Fig.4 : Dimensionless turbulent heat flux $-v\theta^+$

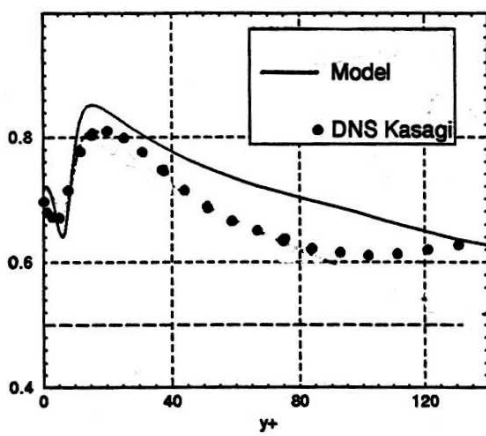


Fig. 5 : Time scales ratio $R = \tau_\theta / \tau$

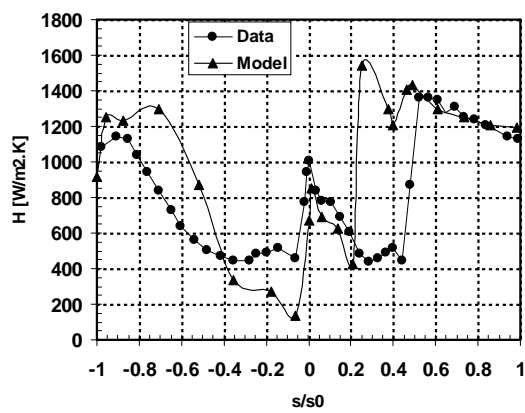


Fig. 6 : Heat transfer coefficient H

This page has been deliberately left blank



Page intentionnellement blanche